Physics of the τ lepton at LEP

Paolo Privitera
Institut für Experimentelle Kernphysik,
Universität Karlsruhe, D-7500 Karlsruhe

INSTITUT FÜR EXPERIMENTELLE KERNPHYSIK
UNIVERSITÄT KARLSRUHE

CERN-PPE/91-185
IEKP-KA/91-09
17 October 1991

Physics of the τ lepton at LEP

Paolo Privitera
Institut für Experimentelle Kernphysik,
Universität Karlsruhe, D-7500 Karlsruhe

Abstract

Recent results of the LEP experiments on the τ lepton properties are reviewed. In particular, the coupling of the τ to Z^0, the measurement of the τ polarization, the branching ratios of the τ and its lifetime are discussed.

(Invited talk at the
XIV International Warsaw meeting on Elementary Particle Physics
May 1991)

1 Introduction

Since its discovery [1] in 1975, the τ lepton has been extensively studied, and its fundamental properties are now established.

The large number of $\tau^+\tau^-$ pairs collected at the LEP collider offer the possibility of a wide range of experimental studies of the τ lepton, with several advantages compared to lower energy machines.

The τ candidates selection is relatively easy, thanks to the typical topologies (Section 2).

The process $Z^0 \rightarrow \tau^+\tau^-$ tests the coupling of the τ lepton to the Z^0 through the measurement of the decay width Γ_τ and the forward-backward asymmetry A_{FB}. It also provides a test of lepton universality (Section 3).

The difference in the coupling of the Z^0 to right-handed and left-handed $\tau^\pm$ produces a small net polarization P_τ. The τ polarization can be experimentally investigated through the τ decay products, and since $P_\tau \propto \sin^2\theta_W$, an independent measurement of the electroweak mixing angle θ_W can be performed (Section 4).

The clean environment of the LEP collider and the particle identification capability of the experiments allow a competitive measurement of the τ branching ratios (Section 5).

At the Z^0 peak, the τ decay lenght is relatively large ($\approx$ 2.2 mm), facilitating the measurement of the τ lifetime (Section 6).

In addition, a massive τ lepton is a preferential candidate to investigate new physics panorama (Section 7).

In the following sections, the recent results on these topics, coming from the data collected by the LEP experiments (ALEPH, DELPHI, L3 and OPAL) in 1990, are reported.

2 Selection of τ events

A typical $Z^0 \rightarrow \tau^+\tau^-$ event, as seen in the DELPHI detector, is shown in Fig. 1. Due to the τ decay properties and its high energy at the Z^0 peak, a $\tau^+\tau^-$ event is nicely characterized by two low multiplicity, back to back jets of particles. The neutrinos coming from τ decays will, in addition, result in a significant missing energy in the event.

On the other hand, possible backgrounds have also clear signatures. Two high momentum tracks ($p_{tot} \approx 2E_{\rm beam}$) with small acollinearity angle characterize a $Z^0 \rightarrow \mu^+\mu^-$ event. A $Z^0 \rightarrow e^+e^-$ event will leave, in addition, a large amount of energy in the electromagnetic calorimeters ($E_{tot} \approx 2E_{\rm beam}$). High multiplicity particle jets coming from the quark hadronisation identify a $Z^0 \rightarrow q\bar{q}$ event. The two-photon processes ($e^+e^- \rightarrow e^+e^-X$) produce particle jets with low momentum and energy, and a large acollinearity angle.

All the LEP experiments are thus able to select $\tau^+\tau^-$ events on the basis of general requirements on:

- multiplicity,
- total energy and momentum,
- acollinearity between the two particle jets,

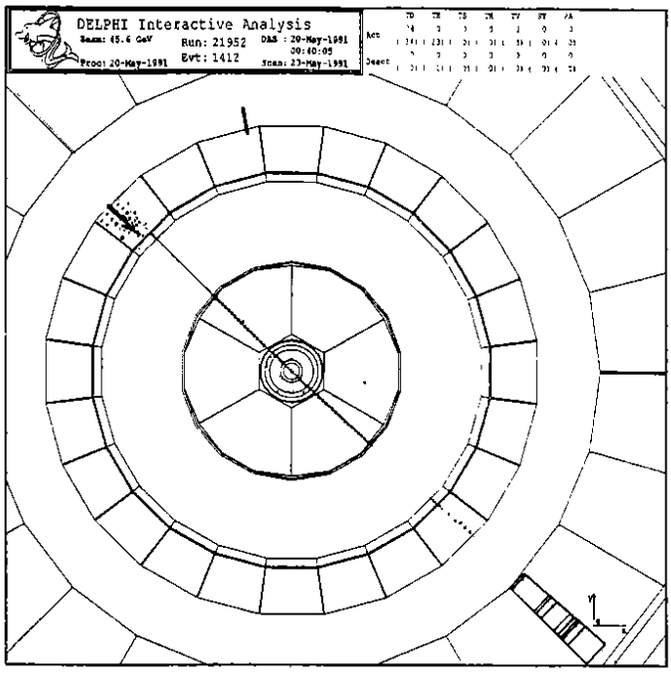

Figure 1: An example of $Z^0 \to \tau^+\tau^-$ event in the DELPHI detector

- some other specific experiment-dependent variables.

Examples of selection criteria are shown in Fig. 2. The trigger efficiency for $Z^0 \to \tau^+\tau^-$ is close to 100%. A total of $\approx$ 16000 $\tau^+\tau^-$ events have been collected in 1990, divided between the different experiments depending on the integrated luminosity given by the machine, the angular region used for the selection and the selection efficiency. The results of the four LEP experiments are summarized in Table 1. It is worthwile noting that the

	$\cos\theta$	Efficiency (%)	Background (%)	Systematic error (%)	Integr. lum. (pb^{-1})	N. events
ALEPH	0.9	86.4	3.0	0.9	7.77	6260
DELPHI	0.7	69.9	1.8	1.2	4.76	2345
L3	0.7	75.4	2.5	2.1	5.11	2540
OPAL	0.9	88.8	2.0	1.3	6.05	4864

Table 1: $Z^0 \to \tau^+\tau^-$ selection efficiency, background subtraction and systematic errors for the four LEP experiments. Efficiencies always refer to the solid angle quoted. The number of selected events and the corresponding integrated luminosity is also shown.

selection efficiency and the background level for $\tau^+\tau^-$ events are a bit worse than the other leptonic channels (typically $\epsilon \approx 90\%$ and *bkg.* $\approx 0.5\%$). This can be easily understood, since practically no $Z^0 \to e^+e^-$ will enter the $Z^0 \to \mu^+\mu^-$ selection (and *vice versa*), while both e^+e^- and $\mu^+\mu^-$ channels constitute a significant background to the τ pairs.

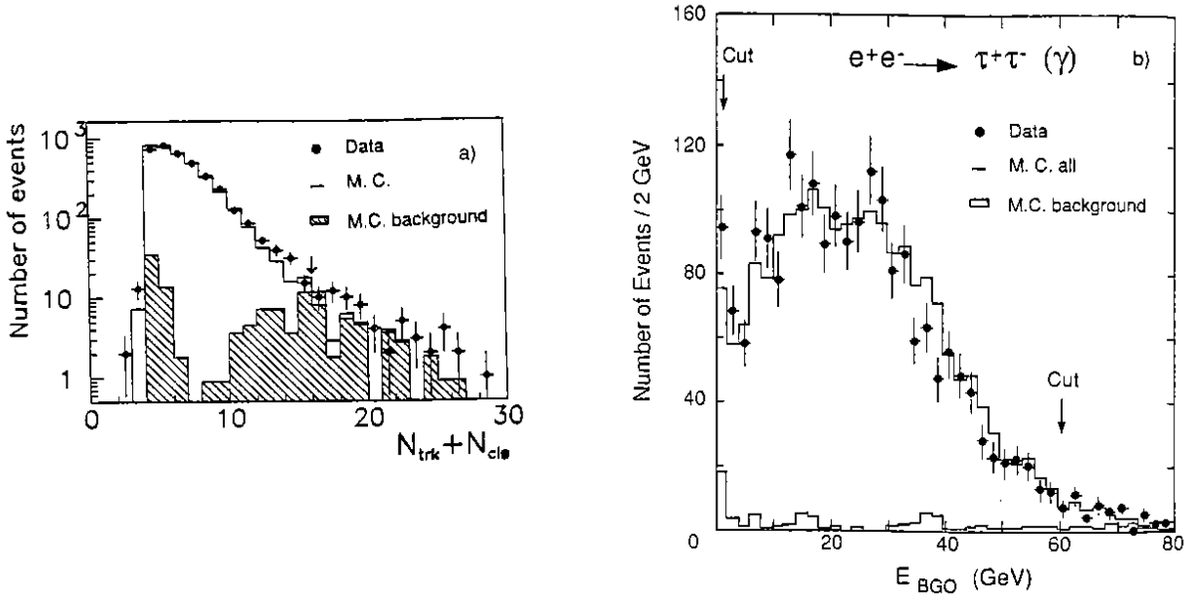

Figure 2: $Z^0 \rightarrow \tau^+\tau^-$ events: examples of selection variables. a) Neutral clusters and charged tracks multiplicity in the OPAL detector; b) total electromagnetic energy in the L3 calorimeter.

The results obtained are already very good, and with increased statistics improvements are foreseen.

3 The Z^0 coupling to τ

It has been known for a long time [2] that electron-positron colliding beam experiments are a privileged laboratory to study the exchange of a neutral weakly interacting vector boson: a strong resonant peak appears in the cross section, and the measurement of its shape parameters allows an unambiguous theoretical interpretation. From this point of view, LEP results represent a great success.

The $Z^0 \rightarrow \tau^+\tau^-$ events are collected at different center of mass energies. The number of events at each energy point is corrected for efficiency and background and converted to a cross section value through the independent luminosity measurement given by the luminosity monitors. The evolution of the cross section with center of mass energy can thus be fitted, according to a model independent parametrization [3], in order to determine the physical parameters (the Z^0 mass, the Z^0 width, etc.). A typical $Z^0 \rightarrow \tau^+\tau^-$ line shape is shown in Fig. 3.

The LEP results [4] for the Z^0 partial width into τ are summarized in Table 2. The hypothesis of a universal lepton coupling is validated comparing the Γ_τ result with the other leptonic partial widths obtained averaging the results of the four experiments ($\Gamma_e = 83.2 \pm 0.5$ MeV, $\Gamma_\mu = 83.4 \pm 0.8$ MeV).

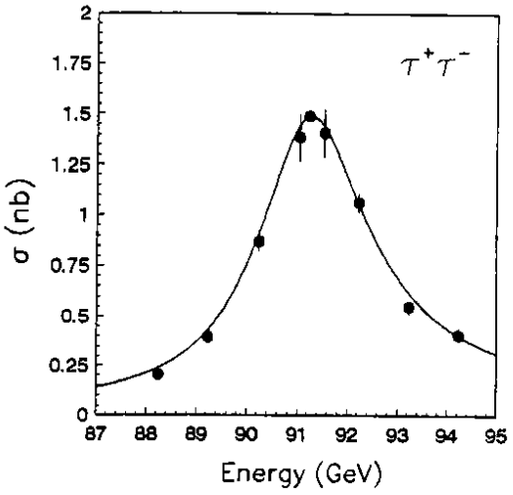

Figure 3: ALEPH $Z^0 \rightarrow \tau^+\tau^-$ line shape

	ALEPH	DELPHI	L3	OPAL	Average LEP
Γ_τ MeV	82.4 ± 1.6	82.7 ± 2.4	84.0 ± 2.7	82.7 ± 1.9	82.8 ± 1.0

Table 2: The $Z^0 \rightarrow \tau^+\tau^-$ partial widths measured by the four LEP experiments from fits of the line shapes.

The production of a fermion-antifermion pair through Z^0 exchange creates an asymmetry in the angular distribution of the outgoing fermion:

$$\frac{d\sigma}{d\cos\theta^*} \propto 1 + \cos^2\theta^* + \frac{8}{3} A_{FB} \cos\theta^*, \tag{1}$$

where θ^* is the angle of the fermion with respect to the electron beam direction and A_{FB} is the forward-backward asymmetry. The A_{FB} can be easily obtained by counting the number of τ^- scattered into the forward (N_F) and backward (N_B) hemisphere

$$A_{FB} \equiv \frac{N_F - N_B}{N_F + N_B}, \tag{2}$$

or with a likelihood fit to the assumed angular distribution described by Eq. (1). Examples of the τ angular distribution and the A_{FB} evolution in function of the center of mass energy are shown in Fig. 4.

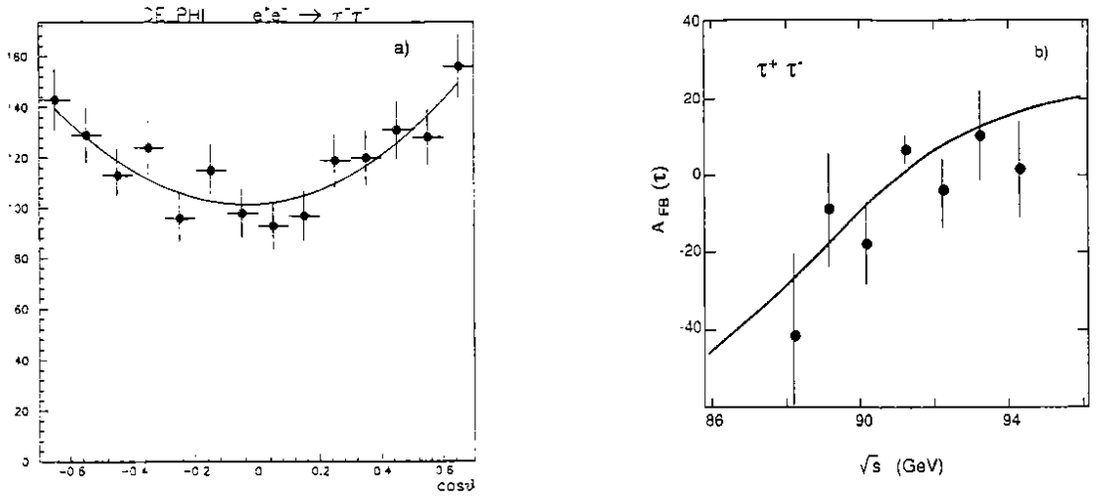

Figure 4: $Z^0 \to \tau^+\tau^-$ forward-backward asymmetry: a) DELPHI τ angular distribution; b) L3 A_{FB} as a function of center of mass energy. The continuous lines represent the fits to the expected distributions.

Constraints on the vector and axial-vector coupling constants can be obtained from A_{FB} which at the peak ($\sqrt{s} = \mathrm{M}_Z$) can be written:

$$A_{FB} \approx 3 \frac{g_V^e g_A^e}{(g_V^e)^2 + (g_A^e)^2} \frac{g_V^\tau g_A^\tau}{(g_V^\tau)^2 + (g_A^\tau)^2} \approx 3 \left(\frac{g_V}{g_A}\right)^2 \tag{3}$$

where the last approximation comes from $g_A^2 \gg g_V^2$ and the assumption of lepton universality. Also the decay width depends on combination of the couplings, through

$$\Gamma_\tau = \frac{G_F M_Z^3}{6\sqrt{2}\pi} \left((g_V^\tau)^2 + (g_A^\tau)^2\right). \tag{4}$$

In principle, a simultaneous fit of the asymmetry and the cross sections provides a determination of g_V^τ and g_A^τ.

From the experimental point of view the A_{FB} measurement is easy, since the actual angular acceptance of the detector is not very important and the only significant systematic error is coming from charge misidentification. However, the statistical error represents a limitation: since $A_{FB} \approx 2\%$ at the pole only with more than 10^5 τ's the measurement is at the level of $\approx 3\sigma$ from zero. An increased statistics will clearly help to get a more precise measurement.

4 The τ polarization

Helicity conservation at high energy has important consequences when applied to the process $e^+e^- \to Z^0 \to \tau^+\tau^-$. A schematic explanation is presented in Fig. 5.

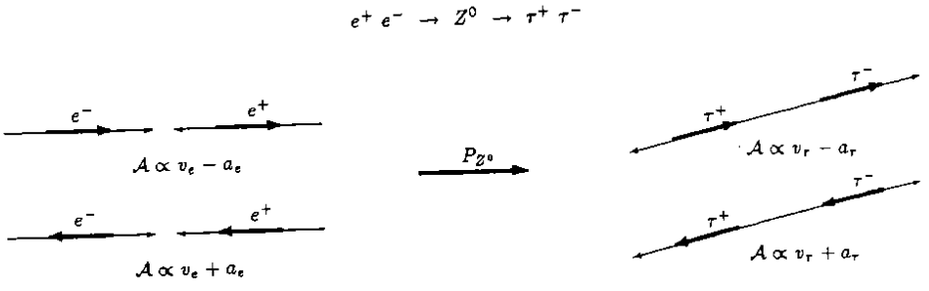

Figure 5: The τ polarization observables. The thin arrows represent particle momenta, the thick ones particle spins.

The two allowed helicity configurations of the electron-positron initial state couple differently to the Z^0, which results in a Z^0 polarization P_Z. In an analogous way, the difference in the coupling of the Z^0 to right-handed and left-handed $\tau^\pm$ produces an average polarization P_τ. The described process produces two observables:

$$P_\tau = \frac{N_- - N_+}{N_- + N_+} = -2\frac{g_V^\tau \cdot g_A^\tau}{(g_V^\tau)^2 + (g_A^\tau)^2}, \qquad A_{FB} = \frac{3}{4} P_Z P_\tau, \tag{5}$$

where P_τ is the longitudinal τ polarization, $N_\pm$ is the number of τ^- with helicity ± 1, and A_{FB} is the forward-backward asymmetry defined in Eq. (3). Note that $P_{\tau+} = -P_{\tau-}$.

The interest in a measurement of the τ polarization stands in the fact that P_τ violates parity and is linear in $g_V \propto 1 - 4\sin^2\theta_W$. The corresponding error on the electroweak parameter is $\Delta \sin^2\theta_W \approx \Delta P_\tau / 8$.

On the contrary, the forward-backward asymmetry is not parity violating, and is quadratic in g_V. This gives an error $\Delta \sin^2\theta_W \approx \Delta A_{FB}/2$.

Given the gain of a factor 4 in the error on $\sin^2\theta_W$ with respect to A_{FB}, even with limited statistics, the measurement of P_τ provides a competitive determination of the electroweak mixing parameter.

4.1 Decays of the τ as polarization analyzers

The decay characteristics of the τ lepton were already established in 1971 by Tsai [5], even before the τ lepton was actually discovered. In particular, it was clear that since τ^+ and τ^- decay via weak interactions where parity conservation is maximally violated, the angular distribution of decay products depends strongly on the spin orientation of the τ. The τ decay works thus as a spin analyzer and gives the unique possibility of determining the τ polarization through the study of the decay products.

To clarify the ideas, it is worthwile to present in some details the simplest case of $\tau^- \to \pi^-\nu_\tau$ [6]. Since this is a two body decay, ν_τ and π^- come out back to back in the τ rest frame, and the component of the orbital angular momentum along the direction of ν_τ is thus zero. Now, ν_τ has a negative helicity, and hence prefers to be emitted opposite to the direction of the spin of τ^-. Therefore, π^- prefers to be emitted in the direction of the spin of the τ^-. A quantitative prediction for the pion angular distribution can be simply derived using quantum mechanics (see Fig. 6), and turns out to be $W_\pm \propto 1 \pm \cos\bar{\theta}$ (for τ helicity ± 1), where $\bar{\theta}$ is the angle between the pion direction and the τ spin quantization axis calculated in the τ rest frame.

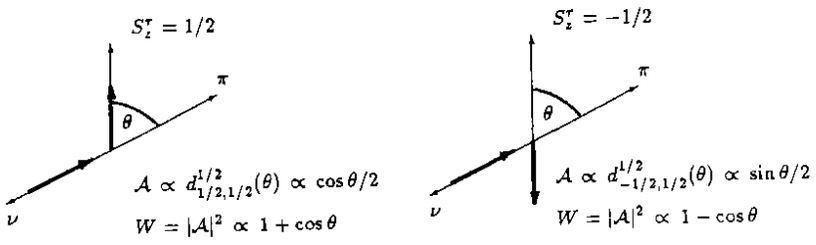

Figure 6: The decay $\tau \to \pi\nu_\tau$ in the τ rest frame. The thin arrows represent particle momenta, the thick ones particle spins. The two pictures correspond to the cases for positive and negative τ helicity.

Summing over the helicity states, the expected pion angular distribution is:

$$\frac{1}{N}\frac{dN}{d\cos\bar{\theta}} = \frac{1}{2}\left(1 + P_\tau \cos\bar{\theta}\right). \tag{6}$$

The Lorentz boost from the τ rest frame to the Laboratory determines a simple relation between the angle $\bar{\theta}_\pi$ and the energy of the pion measured in the Lab:

$$\cos\bar{\theta}_\pi = \frac{4E_\pi m_\tau^2 - 2E_{beam}(m_\tau^2 + m_\pi^2)}{(m_\tau^2 - m_\pi^2)\sqrt{4E_{beam}^2 - 4m_\tau^2}} \approx 2x_\pi - 1, \qquad x_\pi = \frac{E_\pi}{E_{beam}}, \tag{7}$$

where the approximation is valid when terms of the order $(m_\pi/m_\tau)^2$ and $(m_\tau/E_{beam})^2$ are neglected. The sensitivity to P_τ given by the pion angular distribution in the τ rest frame is thus recovered in the Laboratory by taking the pion energy distribution:

$$\frac{1}{N}\frac{dN}{dx_\pi} = 1 + P_\tau(2x_\pi - 1). \tag{8}$$

The lepton energy distribution for the leptonic decays $\tau \to \mu\nu\bar{\nu}, e\nu\bar{\nu}$ is also sensitive to P_τ, but since these are not two body decays, the x_{lept} dependence is more complicated (a third order polynomial) resulting in a lower sensitivity to P_τ.

The hadronic decays $\tau \to \rho\nu, a_1\nu$ are similar to the decay into $\pi\nu$, but now the spin 1 hadron presents both longitudinal and transverse spin states, that give an additional factor α multiplying the $\cos\bar{\theta}$ term of Eq. (6), with $\alpha_\rho \approx 0.46$ and $\alpha_{a_1} \approx 0.12$. The correspondent reduced sensitivity to P_τ can be recuperated by measuring the helicity of the spin 1 hadron through the decay distribution of the hadronic system [7]. A second angle ψ, which characterizes the decay distribution of the hadron into final state pions and is expressed in terms of Laboratory observables, is introduced. For the ρ, this is the decay angle of the 2π system with respect to the ρ line of flight, and is given in terms of the energies of the two pions:

$$\cos\psi = \frac{m_\rho}{\sqrt{m_\rho^2 - 4m_\tau^2}} \quad \frac{E_\pi - E_{\pi^0}}{|\vec{p}_\pi + \vec{p}_{\pi^0}|}, \tag{9}$$

while for the a_1, ψ is the angle between the normal to the decay plane of the 3π system in the a_1 rest frame and the a_1 line of flight. A bidimensional fit to $\cos\bar{\theta}$ and $\cos\psi$ is then performed.

It is interesting to compare the sensitivity to P_τ of the different decay channels. For

Decay mode	$S_X = (\Delta P_\tau\sqrt{N})^{-1}$	B_X	Relative weight $S_X^2 B_X$
$\tau \to \pi\nu$	0.6	0.11	1
$\tau \to \rho\nu$	0.52(0.28)	0.23	1.6
$\tau \to a_1\nu$	0.24(0.07)	0.07	0.1
$\tau \to e\nu\bar{\nu}$	0.22	0.18	0.2
$\tau \to \mu\nu\bar{\nu}$	0.22	0.18	0.2

Table 3: Sensitivity, branching ratio and relative weight for the different τ decay modes. For $\tau \to \rho\nu$ and $\tau \to a_1\nu$ the sensitivity for the two-dimensional fit and, in parenthesis, for the one-dimensional fit are quoted. The relative weights are normalized with respect to the $\tau \to \pi\nu$ channel.

all the decay modes the P_τ dependence can be expressed in a general way as $W(x) = f(x) + P_\tau g(x)$ with $\int f dx = 1$ and $\int g dx = 0$, where f and g are function of a certain variable x (for example a normalised energy). The error on P_τ obtained from a fit to the distribution $W(x)$ is asymptotically given by:

$$\Delta P_\tau = \frac{1}{\sqrt{N}}\left[\int \frac{g^2}{f + P_\tau g} dx\right]^{-\frac{1}{2}} = \frac{1}{S\sqrt{N}}, \tag{10}$$

where N is the number of events contained in the distribution and S represents an ideal sensitivity.

With a given channel X, the error on P_τ is:

$$(\Delta P_\tau)_X = \frac{1}{S_X\sqrt{B_X N_\tau}}, \tag{11}$$

where B_X is the branching ratio of $\tau \to X$. The error obtained combining all the decay modes will thus be:

$$\Delta P_\tau = \frac{1}{\sqrt{\sum_X \frac{1}{\Delta P_X^2}}} = \frac{1}{\sqrt{\sum_X S_X^2 B_X N_\tau}}. \tag{12}$$

The sensitivity S_X, the branching ratio B_X and the correspondent relative weight $S_X^2 B_X$ for the different decay modes are reported in Table 3. One can easily check that the error on P_τ is improved by almost a factor two compared to $\tau \to \pi\nu$ when all the decay modes are combined.

4.2 Experimental aspects of the τ polarization measurement

So far only the theoretical framework of the τ polarization has been discussed. As a matter of fact, the actual measurement represents a real experimental challenge for the LEP detectors. Two fundamental aspects are emphasized in the following.

- **Identification of final states**

  The first step toward a measurement of P_τ is the 'classification' of the τ candidate on the basis of its decay, given the different shape of the experimental distributions depending on the τ decay mode. In this respect, the particle identification capability of the detector is of extreme importance. One requires the identification of

  - e, μ and π $\quad(\tau \to e, \mu, \pi)$,
  - γ and π^0 $\quad(\tau \to \rho \to \pi\pi^0)$.

  This task is complicated by the very dense environment, since the highly energetic τ decays into charged and neutral particles which have a mean separation angle of only a few degrees. A high granularity of the detector is thus expected. Another important point is the understanding of the background. The main contribution comes from the τ decays which are misidentified. One reason is the intrinsic limitation in the particle identification (π/e, π/μ separation). Also, particles which enter parts of the detector which are not sensitive are difficult to identify, and other particles can be lost due to intrinsic thresholds in the detector response. An example is $\tau \to \rho\nu \to \pi\pi^0\nu$. If the π^0 is lost in a detector crack or has a very low energy and is not detected, this event will enter the $\tau \to \pi\nu$ selection. An optimal detector would be sensitive in most of the solid angle and have a low energy threshold. A realistic Monte Carlo representation of the detector is of paramount importance.

- **The experimental energy distribution**

  The τ polarization measurement is essentially given by the fit of the experimental energy distribution of the identified τ decay product with the corresponding

expected theoretical shape. The experimental distribution has to be corrected for different effects. In particular, not only one has to know

- the τ decay identification efficiency,
- the background from misidentified τ decays,

but also their *energy dependence*. The level of understanding that one can get from Monte Carlo and independent real data studies is the limiting factor in the determination of the systematic error on the measurement.

It should now be clear that the P_τ measurement demands a well performing detector apparatus (small dead regions in the detector and low energy thresholds). A detailed understanding of the detector response, the need for a realistic Monte Carlo and the possibility of independent checks of the analysis using real data represent a very difficult task. This should be enough to explain why only recently have final results on the τ polarization been published by some of the LEP experiments.

4.3 Results of the P_τ measurement

The ALEPH, DELPHI and OPAL collaborations have presented practically final results [8] on the τ polarization using 1990 data. In the following, one example for each decay mode will be presented in some detail, in order to give a feeling of how the different detectors have performed their analysis.

- **The $\tau \to \mu\nu\bar{\nu}$ channel**

  The identification of muons in the ALEPH detector is based on the response of the hadron calorimeter. The HCAL is instrumented with 23 layers of streamer tubes, which guarantee a high granularity both in the longitudinal and transverse direction. Penetrating muons leave hits in the outermost layers of HCAL within a few centimeters from the extrapolated track. Pions typically interact earlier, leaving in the HCAL planes a wider hit pattern. The identification efficiency has been estimated from real data, using muons selected independently with the muon chambers. The pion misidentification has been estimated using pions coming from $\tau \to \rho\nu$ events selected with an identified π^0 in the electromagnetic calorimeter. The muon momentum spectrum is shown in Fig. 7.

- **The $\tau \to e\nu\bar{\nu}$ channel**

  Electron identification in the OPAL detector is based on the properties of the electromagnetic calorimeter, made of $\approx$ 9500 lead-glass blocks of 24.6 radiation lengths. The electromagnetic energy associated to an electron candidate is required to be compatible with the measured track momentum, as shown in Fig. 8. The measured electromagnetic energy for the electron candidates is also shown. The selection efficiency determined by Monte Carlo was corrected for the momentum dependence using real data control samples of low energy electrons coming from $e^+e^- \to (e)e\gamma$ and high energy electrons from $e^+e^- \to e^+e^-$.

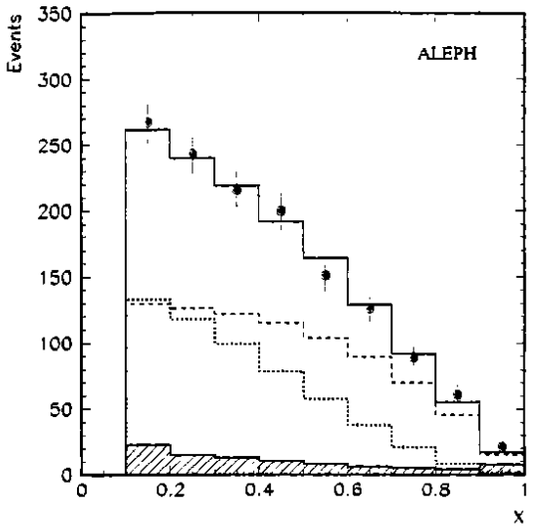

Figure 7: ALEPH $\tau \to \mu\nu\bar{\nu}$. The muon momentum in units of beam momentum, with data (points with error bars), background (shaded histogram), and fitted Monte Carlo distribution (solid line) with components due to positive (dotted line) and negative (dashed line) τ helicities.

- **The $\tau \to \pi\nu$ channel**

  The $\tau \to \pi\nu$ decay mode has to be disentangled from the $\tau \to \mu\nu\bar{\nu}$ channel. In the DELPHI detector the muon chamber and the hadron calorimeter information is used to reject the background. The longitudinal shape of the energy deposition in the HCAL is checked with real data test samples of muons selected with the muon chambers and pions selected from $\tau \to \rho\nu$. The background coming from $\tau \to \pi n\gamma$ is controlled requiring limited activity in the electromagnetic calorimeter around the extrapolated track. Note that the decay $\tau \to K\nu$ is contained in the selected events, since no attempt is done to make π/K separation. The $\tau \to \pi\nu$ energy spectrum corrected for efficiency and background is shown in Fig. 9.

- **The $\tau \to \rho\nu$ channel**

  The ρ decays into a charged pion and a π^0. The π^0 decays into two photons, which are seen in the electromagnetic calorimeter as two neutral clusters or only one cluster in case the π^0 has high energy. The invariant mass of the two photons in the ALEPH detector (Fig. 10) shows a nice peak corresponding to the π^0 mass. A clear ρ peak is also visible in the invariant mass between the two-photons reconstructed π^0 (or a single neutral cluster candidate π^0 with energy greater than 4 GeV) and the charged track.

- **The $\tau \to a_1\nu$ channel**

  ALEPH has studied this channel looking at three prongs events. A sample of events with three charged tracks and at least one photon was also selected to study the background. The invariant mass of the three charged tracks is shown in Fig. 11.

The essential features of the analysis of the different decay channels for the ALEPH, DELPHI and OPAL collaborations are summarized in Table 4. Combining all LEP results,

ALEPH	$\cos\theta$	Acceptance (%)	Background (%)	N. events	P_τ
$\tau \to \mu\nu\bar{\nu}$	0.9	52	3.7	1401	$-0.19 \pm 0.13 \pm 0.06$
$\tau \to e\nu\bar{\nu}$	0.7	52	2.5	843	$-0.36 \pm 0.17 \pm 0.06$
$\tau \to \pi\nu$	0.9	43	6	805	$-0.130 \pm 0.065 \pm 0.044$
$\tau \to \rho\nu$	0.9	58	10.5	2184	$-0.124 \pm 0.047 \pm 0.051$
$\tau \to a_1\nu$	0.9	64	6.5	990	$-0.15 \pm 0.15 \pm 0.07$
all channels					-0.152 ± 0.045
g_V^τ/g_A^τ					0.076 ± 0.023
$\sin^2\theta_W$					0.2302 ± 0.0058
DELPHI	$\cos\theta$	Acceptance (%)	Background (%)	N. events	P_τ
$\tau \to \mu\nu\bar{\nu}$	0.7	56	3	686	$-0.09 \pm 0.19 \pm 0.10$
$\tau \to e\nu\bar{\nu}$	0.7	48	3	590	$-0.10 \pm 0.20 \pm 0.09$
$\tau \to \pi\nu$	0.7	42	10	320	$-0.28 \pm 0.10 \pm 0.08$
$\tau \to \rho\nu$	0.7	46	18	730	$-0.170 \pm 0.085 \pm 0.080$
all channels					-0.176 ± 0.076
g_V^τ/g_A^τ					0.089 ± 0.038
$\sin^2\theta_W$					0.227 ± 0.009
OPAL	$\cos\theta$	Acceptance (%)	Background (%)	N. events	P_τ
$\tau \to \mu\nu\bar{\nu}$	0.7	76	3	903	$-0.17 \pm 0.16 \pm 0.10$
$\tau \to e\nu\bar{\nu}$	0.7	74	5.7	964	$+0.20 \pm 0.13 \pm 0.08$
$\tau \to \pi\nu$	0.7	35	6	309	$-0.08 \pm 0.10 \pm 0.07$
all channels					-0.01 ± 0.09
g_V^τ/g_A^τ					0.01 ± 0.04
$\sin^2\theta_W$					0.237 ± 0.009

Table 4: The P_τ measurement in ALEPH, DELPHI and OPAL: the angular range, the acceptance, the background fraction, the number of selected events, and the fitted values of P_τ for the selected τ decay modes. The quoted acceptance contains the channel identification efficiency folded with the $\tau^+\tau^-$ selection efficiency, normalized to the selected angular range. The first error quoted on P_τ is statistical, the second is systematic. The value obtained combining all the decay modes is also reported, together with the correspondent value for the ratio of the τ coupling constants and the electroweak mixing parameter.

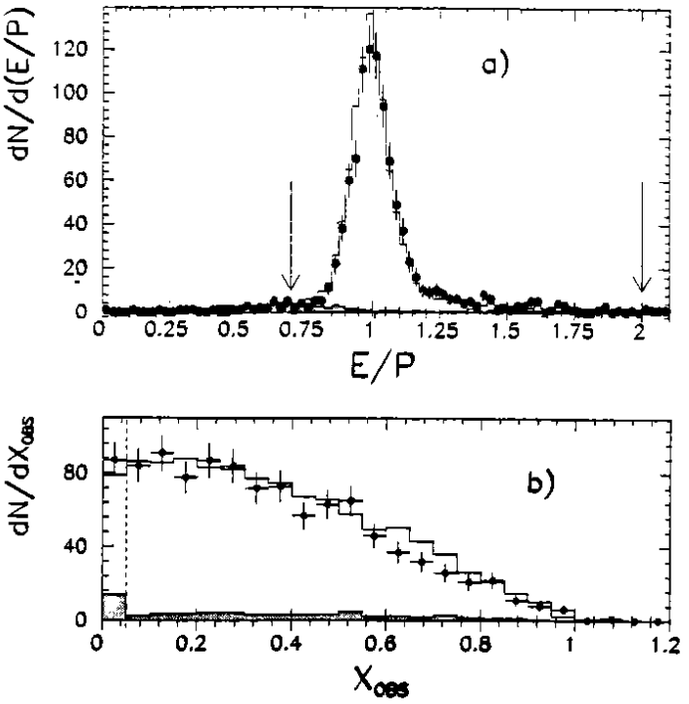

Figure 8: OPAL $\tau \to e\nu\bar{\nu}$. In a) the energy divided by the momentum for the $\tau \to e\nu\bar{\nu}$ candidates. The arrows indicate the cuts used for the selection. The distribution of measured energy in units of beam momentum is shown in b). The data are indicated by the points with error bars, the expected signal from Monte Carlo by the open histogram, and the expected background from Monte Carlo by the shaded histogram.

the mean value obtained is $P_\tau = -0.135 \pm 0.035$, indicating a parity violation[1] in the process $e^+e^- \to \tau^+\tau^-$. The result corresponds to a ratio of the neutral current vector and axial vector coupling constants $g_V^\tau/g_A^\tau = 0.068 \pm 0.018$ and a value of the electroweak mixing parameter $\sin^2\theta_W = 0.2323 \pm 0.0045$. This value of g_V^τ/g_A^τ can be combined with the measurement of the $Z^0 \to \tau^+\tau^-$ partial width at LEP, $\Gamma_\tau = 82.8 \pm 1.0$ MeV, to separate g_V^τ and g_A^τ, using Eq. (4). Assuming g_A^τ is negative, one obtains:

$$g_V^\tau = -0.034 \pm 0.009,$$

$$g_A^\tau = -0.498 \pm 0.003.$$

This determination by LEP of the vector and axial vector τ coupling constants improves the accuracy by more than one order of magnitude compared to previous results obtained at lower energies [12] and the measurement is still limited by the present statistics.

[1]Note that parity violation in the weak neutral current has been observed so far only in polarized electron inelastic scattering [9] and in atomic transitions [10]. Recently, parity violation in the decay $\tau \to 3\pi\nu$ has been reported [11].

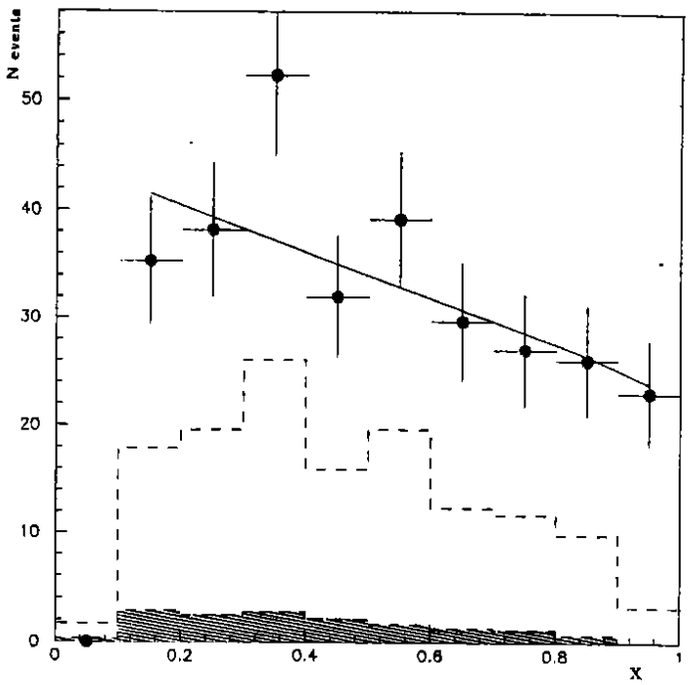

Figure 9: DELPHI $\tau \to \pi\nu$. The final momentum distribution for the $\tau \to \pi\nu$ candidates. The points with error bars are the corrected spectrum together with the fit. The data spectrum before correction is represented with the dashed line and the background with the shaded histogram (both are scaled by a factor 0.4).

5 The τ branching ratios

The experimental situation [13] on the τ branching fractions presents quite interesting aspects, since several discrepancies exist among different investigations. A striking feature is the so called 'one-prong problem': the sum of the exclusive branching ratios B_i for exclusive one-prong channels is smaller than the corresponding one-prong inclusive fraction (B_i^T). The difference is of the order of 4%.

The ALEPH collaboration has presented [14] a very detailed analysis on both topological and exclusive τ branching ratios using data collected in 1989 and 1990. The charged track topology of a $\tau^+\tau^-$ event should be ij (i,j = 1, 3, 5). However some tracks can be lost because they overlap, escape detection or interact, and some additional tracks can appear from converted photons or hadron interactions. Thus, the $\tau^+\tau^-$ event topology will be kl (k,l = 1, 2,...) instead of ij. The number of $\tau^+\tau^-$ candidates n_{kl} expected to be seen in the detector with topology kl is related to the true number of $\tau^+\tau^-$ pairs N_{ij} with topology ij by:

$$n_{kl} = n_{kl}^{bkg} + \sum_{i \le j} T_{ij \to kl} N_{ij} \quad (k,l = 1,2,3,...), \tag{13}$$

$$N_{ij} = (2 - \delta_{ij}) N_{\tau^+\tau^-} B_i^T B_j^T \quad (i,j = 1,3,5), \tag{14}$$

where $N_{\tau^+\tau^-}$ is the total number of produced $\tau^+\tau^-$ pairs, B_i^T is the topological branching ratio for the decay into i charged particles, $T_{ij \to kl}$ is the probability of reconstructiong a

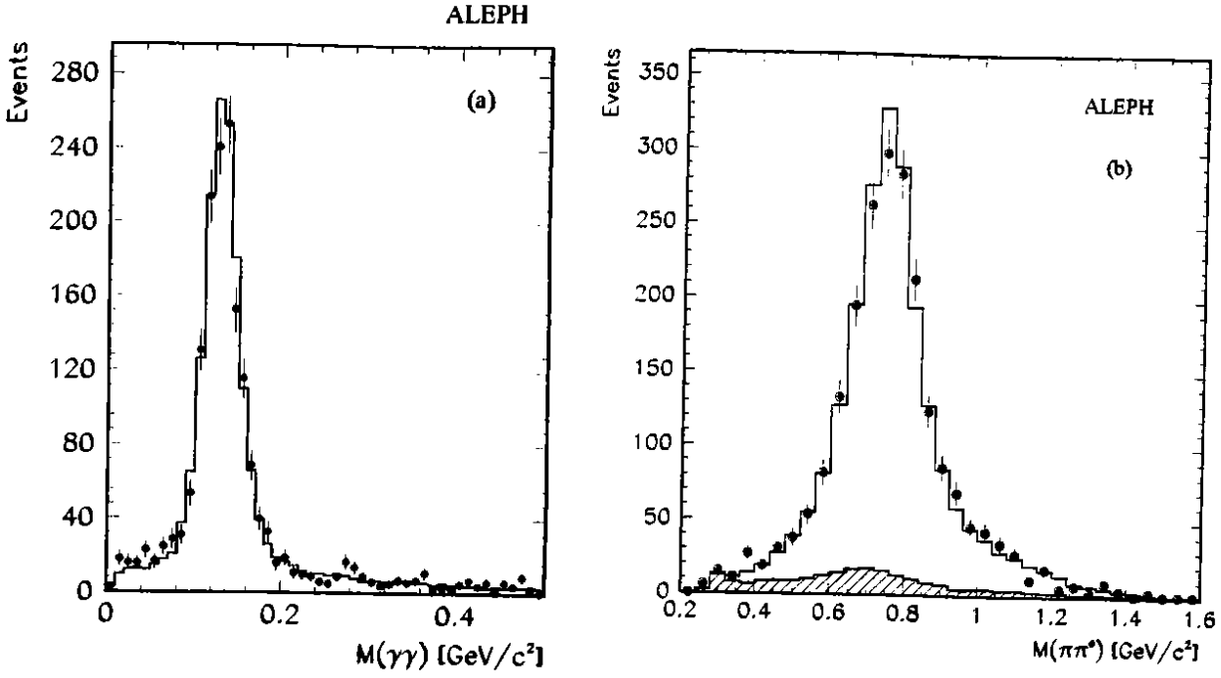

Figure 10: ALEPH $\tau \to \rho\nu$: a) the $\gamma\gamma$ invariant mass in τ candidates with two photons; b) invariant mass of $\pi^{\pm}\pi^0$. Points with error bars represent data, the histogram is the Monte Carlo prediction, and the shaded histogram is the expected background.

kl topology from a ij true topology and n_{kl}^{bkg} is the number of background events with kl topology. A likelihood fit to the observed distribution of multiplicities is used to determine the topological branching ratios:

$$\begin{aligned} B_1^T &= (85.45^{+0.69}_{-0.73} \pm 0.41)\%, \\ B_3^T &= (14.35^{+0.40}_{-0.45} \pm 0.23)\%, \\ B_5^T &= (0.105^{+0.05}_{-0.04} \pm 0.03)\%. \end{aligned} \tag{15}$$

A common relative uncertainty of $\pm 0.47\%$ should be added to take into account the normalization of the $\tau^+\tau^-$ sample. To determine the quoted branching fractions ALEPH has chosen an absolute normalization for the $\tau^+\tau^-$ pair production, calculating the expected number of pairs from the ratio of the hadronic to muonic and electronic Z^0 widths, assuming lepton universality. The advantage of an absolute normalization stands in the possibility of investigating peculiar decay modes that would not be selected in the τ analysis. One could imagine that a τ decayed into eN, where N is a neutrino kind of particle,

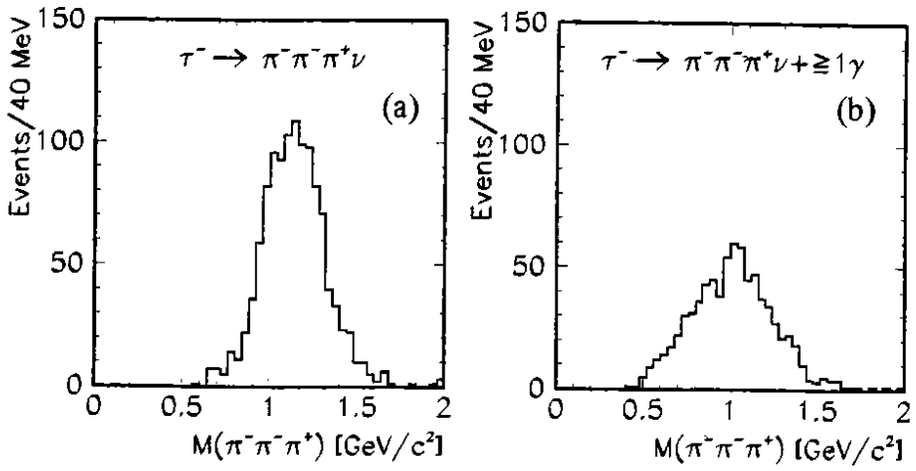

Figure 11: ALEPH: 3π invariant mass for events without reconstructed photons (a) and with at least one reconstructed photon (b).

with almost the same τ mass, and the low momentum electron escapes detection. Assuming lepton universality, the branching ratio of undetected τ decay modes is limited by:

$$B_{undetected} < 2\% \qquad (95\% \quad CL).$$

ALEPH has also performed a 'quasi-exclusive' branching ratios measurement. The detector capability of identifying e, μ and π, together with γ and π^0 is used to divide the τ decays into 8 classes, as shown in Table 5. The sum of the measured branching ratios is

Class	X for $\tau \to X\nu_\tau$	particle type	number of photons	$B_i(\%)$
1	$e\bar{\nu}_e$	$\geq 1e$	any	$18.09 \pm 0.45 \pm 0.41$
2	$\mu\bar{\nu}_e$	$1\ \mu$	any	$17.35 \pm 0.41 \pm 0.33$
3	h	1 hadron	0	$13.32 \pm 0.44 \pm 0.30$
4	$h\pi^0$	1 hadron	1, 2 with 1 π^0	$25.02 \pm 0.64 \pm 0.84$
5	$h2\pi^0$	1 hadron	2, 3 with 1 π^0 4 with 2 π^0	$10.53 \pm 0.66 \pm 0.81$
6	$h \geq 3\pi^0$	1 hadron	3, 4 with 1 π^0, ≥ 5	$1.53 \pm 0.40 \pm 0.46$
7	$3\ h$	≥ 2 hadrons	0	$9.49 \pm 0.36 \pm 0.62$
8	$3\ h \geq 1\pi^0$, $5\ h \geq 0\pi^0$	≥ 2 hadrons	≥ 1	$5.05 \pm 0.29 \pm 0.65$

Table 5: ALEPH quasi exclusive branching ratios measurement: the selection criteria in terms of the identification of the charged track and the number of photons and π^0 are given for each generic class. A common relative uncertainty of 1% should be added to the quoted branching ratios errors to take into account the normalization of the τ sample.

consistent with 100%:

$$\sum_{i=1}^{8} B_i = 100.4 \pm (1.3)_{stat} \pm (0.8)_{sys} \pm (1.0)_{norm}\%,$$

and, in particular, the sum of all one-prong channels is $85.8 \pm 1.6\%$, consistent with the corresponding topological branching ratio given in Eq. (15). An exclusive analysis has also been performed, requiring a positive identification of the π^0. No evidence for decays producing photons beyond the expected modes with π^0 is found, and a limit of 3.7% at 95% confidence level can be set on the branching ratio of new photonic decay modes. The ALEPH results, thus, show no evidence for the 'one-prong problem', confirming the recent analysis of the CELLO collaboration [15]. It is interesting to note that both experiments have measured a larger branching fraction for the modes $\tau \rightarrow 3\pi\nu_\tau, \pi 2\pi^0\nu_\tau$ as compared to previous determinations.

The L3 collaboration has also measured the topological branching ratios [16]:

$$B_1^T = (85.6 \pm 0.6 \pm 0.3)\%,$$

$$B_3^T = (14.4 \pm 0.6 \pm 0.3)\%,$$

$$B_5^T < 0.34\% \quad (95\% \quad CL).$$

These values are consistent with the ALEPH determination and the world averages. Note that, in the L3 case, the branching ratios are determined without an absolute normalization, that is they are normalized to the total number of τ events selected.

The results on some exclusive channels from L3 [16] and OPAL [17] are shown in Table 6.

Decay channel	L3	OPAL
$\tau \rightarrow \mu\nu\bar{\nu}$	$0.175 \pm 0.007 \pm 0.008$	$0.168 \pm 0.005 \pm 0.004$
$\tau \rightarrow e\nu\bar{\nu}$	$0.177 \pm 0.007 \pm 0.006$	$0.174 \pm 0.005 \pm 0.004$
$\tau \rightarrow \pi(K)\nu$	-	$0.121 \pm 0.007 \pm 0.005$

Table 6: L3 and OPAL exclusive branching ratio measurements.

6 The τ lifetime

The tau lepton is a fundamental constitutent of the Standard Model and its lifetime is an important quantity which can be used to test the predictions of the model. In particular, the property of lepton universality can be tested using the relationship:

$$\tau_\tau = \tau_\mu \left(\frac{\mathrm{G}_\mu}{\mathrm{G}_\tau}\right)^2 \left(\frac{\mathrm{m}_\mu}{\mathrm{m}_\tau}\right)^5 \times \mathrm{BR}\left(\tau^- \rightarrow e^-\bar{\nu}_e\nu_\tau\right) \tag{16}$$

where $\tau_{\mu,\tau}$ and $\mathrm{m}_{\mu,\tau}$ are the lifetimes and masses of the muon and tau respectively and $\mathrm{G}_{\mu,\tau}$ are the Fermi constants determined from muon and tau decay. A high precision

measurement of the τ lifetime could clarify the present experimental situation: the world average value of the τ lifetime is 0.303 ± 0.008 ps, which, using Eq. (16), corresponds to $\mathrm{BR}(\tau^- \to e^- \bar{\nu}_e \nu_\tau) = 18.9 \pm 0.5\%$, to be compared with the world average $17.5 \pm 0.5\%$.

A clear advantage for the measurement at LEP is the fact that the τ travels for ≈ 2.2 mm before decaying. Two independent methods have been used.

- **The impact parameter method**

  For one-prong τ decays, the signed impact parameter is the distance of closest approach of the extrapolated track to the production point in the $r\phi$ plane. The sign is taken as positive if the extrapolated track intersects the τ direction before the point of closest approach and as negative otherwise (see Fig. 12). If the geometry

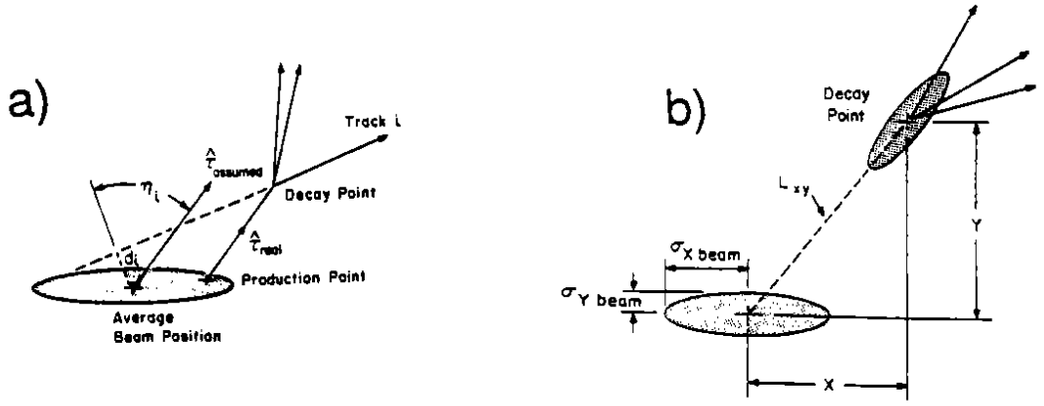

Figure 12: Measurement of the τ lifetime: a) the impact parameter method, b) the decay lenght method.

of the production and decay could be reconstructed perfectly, the impact parameter would always be positive. The negative values are a consequence of the experimental resolution and uncertainties in the τ direction, but its statistical distribution retains sensitivity to the τ lifetime.

The thrust axis of the event is used to determine the τ direction required for the sign of the impact parameter. This axis approximates the actual τ direction with a precision of $\approx 1^o$. The production point of the τ's is taken as the centre of the interaction region measured for each LEP fill by reconstructing the vertices of Z^0 decays to multihadrons.

An event probability density p proportional to the theoretical distribution folded with a gaussian resolution is used for an unbinned maximum likelihood fit to the average impact parameter δ:

$$p(\delta_i) = \frac{1}{\sqrt{2\pi}\sigma_i \delta} \int_0^\infty \exp -\frac{x}{\delta} \exp -\frac{(x-\delta_i)^2}{2\sigma_i^2} dx, \qquad (17)$$

where δ_i is the track impact parameter and σ_i its error. The conversion between the measured average impact parameter and the actual τ lifetime is determined using Monte Carlo τ events generated for different values of the lifetime. In this respect, it is fundamental that the Monte Carlo generated impact parameter distribution is convoluted with a resolution function which takes into account the smearing

due to the finite beam interaction region and the tracking detector experimental resolution. The resolution function can be extracted directly from the data, using $e^+e^- \rightarrow \mu^+\mu^-, e^+e^-$. The impact parameter experimental resolution σ_{exp} can be determined from the r.m.s. σ_d of the $\mu^+\mu^-$ (or e^+e^-) 'missing distance', that is the distance d between the two tracks at the production vertex. Since one knows that the two tracks originate from one point, the experimental resolution on the distance of closest approach is given by $\sigma_{exp} = \sigma_d/\sqrt{2}$. For lower momentum tracks, a small additional contribution comes from multiple scattering in the beam pipe. This can be parametrized as a function of the track momentum p by $\sigma_{msc} = \alpha/p$, where α is typically of the order of 100 μm. The impact parameter distribution of the muons and electrons with respect to the production point measures the projected size of the beam spot folded with the resolution in δ. Subtracting in quadrature σ_{exp}, a typical beam spot size of $\sigma_x \approx 200$ μm in the horizontal direction and of $\sigma_y \approx 20$ μm in the vertical direction is obtained. The total error on the measured distance of closest approach can, thus, be written as:

$$\sigma_\delta^2 = \sigma_{exp}^2 + \sigma_{msc}^2 + \sigma_x^2 \sin^2\phi + \sigma_y^2 \cos^2\phi, \tag{18}$$

where ϕ is the azimuthal angle of the track. For a τ lifetime of ≈ 0.3 ps, an average impact parameter of ≈ 60 μm is expected.

- **The decay length method**

  When the τ decays into three charged tracks, the decay secondary vertex and its distance from the $\tau^+\tau^-$ production point can be determined (see Fig. 12). In the $r\phi$ plane, the three tracks parameters are used to determine the decay vertex position, and the distance d_i from the center of the beam spot is calculated. The laboratory decay distance D_i is, then, given by:

$$D_i = \frac{d_i}{\sin\theta_i}, \tag{19}$$

  where θ_i is the polar angle of the τ taken as that of the thrust axis of the three charged particles in the decay. The sign of the decay distance is defined such that the decay vertices in the τ production hemisphere have a positive sign and those in the opposite hemisphere a negative sign. An unbinned maximum likelihood fit is then performed in order to obtain the average decay length D, as was done for the impact parameter method. The τ lifetime is thus calculated:

$$\tau_\tau = \frac{D}{\beta\gamma c}. \tag{20}$$

  The error on the individual decay length takes into account the contributions from both the size of the beam spot and the error of the reconstructed vertex along the thrust axis, typically 2 mm depending on the decay opening angle (note that the average decay lenght is 2.2 mm).

The DELPHI and L3 collaborations have published results on the τ lifetime [18] applying both methods to the 1990 data. The DELPHI result is based on the good performance of

the microvertex detector, which consists of two concentric layers of silicon-strip detectors at radii of 9 and 11 cm respectively, giving full azimuthal coverage in the polar angle region $43^o < \theta < 137^o$. Each layer has 24 sectors with a 10% overlap in ϕ. A τ event as seen in the inner tracking part of the DELPHI detector is shown in Fig. 13. The

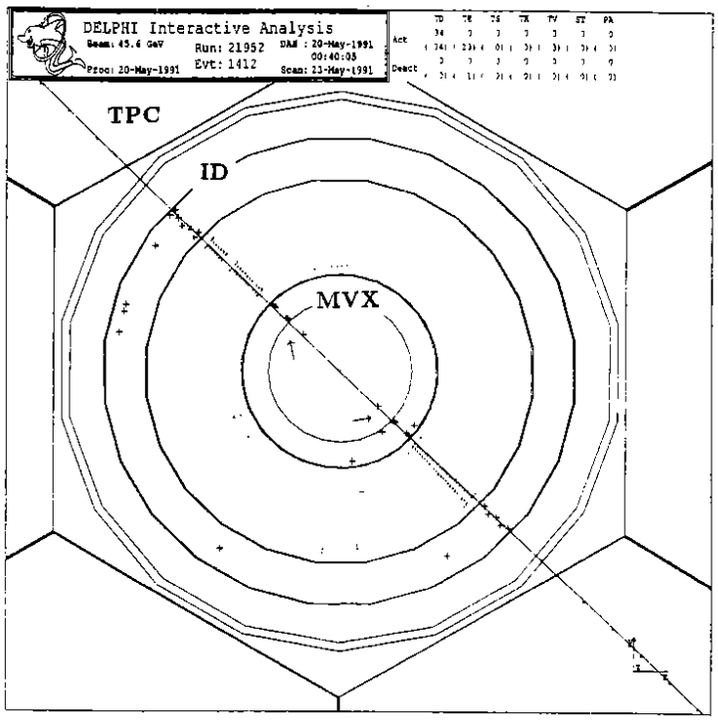

Figure 13: The DELPHI tracking system: the TPC, the Inner Detector and the microvertex detector. The arrows indicate the hits in the microvertex detector. The event shown was taken in 1991 with the three layer configuration.

experimental resolution on the impact parameter, determined with the 'missing distance' in $e^+e^- \rightarrow \mu^+\mu^-$, is 62 μm. In Fig. 14 the impact parameter distribution is shown. The τ lifetime value with the impact parameter method is:

$$\tau_\tau = 0.321 \pm 0.036(stat) \pm 0.016(sys) \text{ ps},$$

where the systematic error is coming mainly from the uncertainty in the resolution function parameters due to the $Z^0 \rightarrow \mu^+\mu^-$ statistics (0.014 ps). The τ lifetime value with the decay length method is:

$$\tau_\tau = 0.310 \pm 0.031(stat) \pm 0.009(sys) \text{ ps},$$

where the systematic error is coming mainly from the uncertainty in the extrapolation resolution (0.008 ps).

The TEC chamber is the tracking device used for the τ lifetime measurement by the L3 collaboration. The experimental resolution on the impact parameter, determined with the 'missing distance' in $e^+e^- \rightarrow e^+e^-, \mu^+\mu^-$, is 144 μm. In Fig. 14 the decay distance distribution is shown. The τ lifetime value with the impact parameter method is:

$$\tau_\tau = 0.318 \pm 0.028(stat) \pm 0.037(sys) \text{ ps},$$

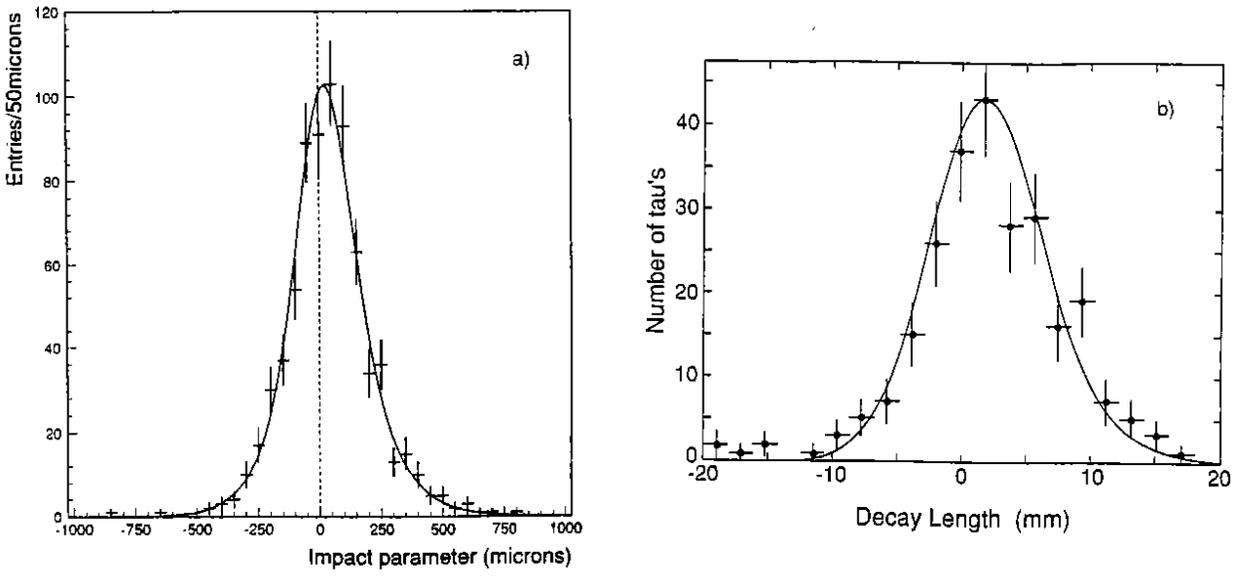

Figure 14: The τ lifetime. a) DELPHI: the impact parameter distribution; b) L3: the decay length distribution.

where the systematic error is coming mainly from the uncertainty in the track parameters errors (0.026 ps). The τ lifetime value with the decay length method is:

$$\tau_\tau = 0.302 \pm 0.036(stat) \pm 0.021(sys) \text{ ps.}$$

The impact parameter and decay length method are statistically independent and, once common systematic errors are taken into account, they can be combined. The DELPHI and L3 results on the τ lifetime, obtained combining the two methods, are compared with recent measurements of other experiments in Table 7. The increasing statistics and detectors upgrades leave large room for improvements. An example is given by the DELPHI microvertex: a third layer has been installed at 6 cm radius in 1991, and the impact parameter resolution has improved by a factor ≈ 3 ($\sigma_{exp} \approx 20$ μm) [19].

7 Other topics

Several searches for new kind of τ leptons, from the excited to the supersymmetric, have been performed at LEP. The Higgs particle coupling to τ has also been investigated. All the searches have been without success[2] so far. In april 1991 the ALEPH collaboration has published a paper [20] claiming a possible excess in the τ channel in events with two leptons and an additional pair of charged particles (V). In a sample of 200000 Z^0 decays, 35 l^+l^-V events were identified, divided in 10 e^+e^-V, 10 $\mu^+\mu^-V$ and 15 $\tau^+\tau^-V$, while the

[2]Other speakers in this Conference have reported detailed results.

Tau Lifetime (ps)					Experiment
0.295	±	0.014	±	0.011	ARGUS
0.325	±	0.014	±	0.018	CLEO
0.299	±	0.015	±	0.010	HRS
0.309	±	0.017	±	0.007	MAC
0.288	±	0.016	±	0.017	MARK II
0.306	±	0.020	±	0.014	TASSO
0.301	±	0.029			JADE
0.314	±	0.023	±	0.009	DELPHI
0.309	±	0.023	±	0.030	L3

Table 7: The DELPHI and L3 results on the τ lifetime, obtained combining the impact parameter and decay length method, compared with recent measurements of other experiments.

expectation from electroweak processes was 3.2 $\tau^+\tau^- V$ in a total of 17 $l^+l^- V$. The features of the events are consistent with the radiation of virtual photons. The Poisson probability of observing 15 events or more events out of a fixed total of 35 is $4 \cdot 10^{-3}$, also taking into account the systematic error on the relative efficiencies. This result is not confirmed by the new analyses [21] of the ALEPH, DELPHI and OPAL collaborations. Including the new data the statistical significance of the excess in the τ channel is significantly reduced: 23 events are found when 16 are expected out of a total of 79.

8 Conclusions

The successful operation of the LEP collider has given $\approx$ 16000 $\tau^+\tau^-$ pairs to the LEP experiments. The selection of the $Z^0 \rightarrow \tau^+\tau^-$ is performed with high efficiency and low background.

The $Z^0 \rightarrow \tau^+\tau^-$ partial width has been measured with high precision:

$$\Gamma_\tau = 82.8 \pm 1.0 \quad MeV \qquad (LEP \quad average).$$

The measurement of the τ polarization has been successfully performed:

$$P_\tau = -0.135 \pm 0.035 \qquad (LEP \quad average),$$

indicating a parity violation in the process $e^+e^- \rightarrow \tau^+\tau^-$.

The result corresponds to a ratio of the neutral current vector and axial vector coupling constants $g_V^\tau/g_A^\tau = 0.068 \pm 0.018$ and a value of the electroweak mixing parameter $\sin^2\theta_{l^+} = 0.2323 \pm 0.0045$. Combining this value of g_V^τ/g_A^τ with the measurement of the $Z^0 \rightarrow \tau^+\tau^-$ partial width at LEP:

$$g_V^\tau = -0.034 \pm 0.009,$$

$$g_A^\tau = -0.498 \pm 0.003,$$

with an improvement of more than one order of magnitude with respect to previous measurements.

The τ topological and exclusive branching fractions have been determined by some of the LEP experiments. In particular, ALEPH do not find any evidence for the debated 'one-prong problem'.

Measurements of the τ lifetime have been performed, with errors already comparable to previous experiments.

No evidence for new physics connected with the τ lepton has been found so far. In particular, the claim by the ALEPH collaboration for a possible excess in the τ channel in events with two leptons and an additional pair of charged particles, has lost most of its significance with the analysis of new data.

It is foreseen that all these results should be significantly improved in the near future, thanks to the increased statistics and detector improvements.

9 Acknowledgements

The author thanks all the collegues who kindly helped in the preparation of the talk and the manuscript. The help of L. Rolandi, D. Reid, H. S. Chen and K. Riles is particularly acknowledged.

References

[1] M. L. Perl et al., Phys. Rev. Lett. 35 (1975) 1489.

[2] N. Cabibbo and R. Gatto, Phys. Rev. 124 (1961) 1577.

[3] F. A. Berends, "Z Physics at LEP 1", eds. G. Altarelli et al., CERN Report CERN-89-08;
A. Borrelli et al., Nucl. Phys B 333 (1990) 357;
M. Martinez et al., Z. Phys. C 49 (1991) 645.

[4] ALEPH Collab., CERN preprint CERN-PPE/91-105 (1991);
DELPHI Collab., CERN preprint CERN-PPE/91-95 (1991);
B. Adeva et al., L3 Collab., Z. Phys. C 51 (1991) 179;
OPAL Collab., CERN preprint CERN-PPE/91-67 (1991).

[5] Y. S. Tsai, Phys. Rev. D 4 (1971) 2821.

[6] A detailed description of the different τ decay channels can be found in:
A. Rouge, Proceedings of the Workshop on τ lepton physics, Orsay (1990), eds. M. Davier and B. Jean-Marie, Editions Frontières (1991).

[7] K. Hagiwara, A. D. Martin, D. Zeppenfeld, Phys. Lett. B 235 (1990) 198;
A. Rougé, Z. Phys C 48 (1990) 75.

[8] D. Decamp et al., ALEPH Collab., Phys. Lett. B 265 (1991) 430;
DELPHI Collab., Contrib. to "International Lepton-Photon Symposium and Europhysics Conference on High Energy Physics", Geneva 1991, and preprint DELPHI 91-60 PHYS 115 (1991);
M. Z. Akrawy et al., OPAL Collab., Phys. Lett. B 266 (1991) 201.

[9] C. Prescott et al., Phys. Lett. B 77 (1978) 347.

[10] L. M. Barkov, M. S. Zolotorev, JETP Lett. 31 (1978) 357; Phys. Lett. B 85 (1979) 308.

[11] ARGUS Collab., H. Albrecht et al., Phys. Lett. B 250 (1990) 164.

[12] S. Odaka, Proceedings of the Workshop on τ lepton physics, Orsay (1990), eds. M. Davier and B. Jean-Marie, Editions Frontières (1991); see also KEK preprint 90-164 (1990).

[13] A detailed review of τ decays can be found in the Proceedings of the Workshop on τ lepton physics, Orsay (1990), eds. M. Davier and B. Jean-Marie, Editions Frontières (1991).

[14] M. Davilov, ALEPH Collab., Contrib. to "International Lepton-Photon Symposium and Europhysics Conference on High Energy Physics", Geneva 1991.

[15] H. J. Behrend et al., (CELLO Collab.), Z. Phys. C 46 (1990) 537.

[16] B. Adeva et al., L3 Collab., Phys. Lett. B 265 (1991) 451.

[17] OPAL Collab., see ref. [8].

[18] P. Abreu et al., DELPHI Collab., Phys. Lett. B 267 (1991) 422;
L3 Collab., see ref. [16].

[19] R. Mc Nulty, private communication.

[20] D. Decamp et al., ALEPH Collab., Phys. Lett. B 263 (1991) 112.

[21] S. L. Wu, ALEPH Collab., Contrib. to "International Lepton-Photon Symposium and Europhysics Conference on High Energy Physics", Geneva 1991;
M. Pimenta, DELPHI Collab., Contrib. to "International Lepton-Photon Symposium and Europhysics Conference on High Energy Physics", Geneva 1991;
M. Roney, OPAL Collab., Contrib. to "International Lepton-Photon Symposium and Europhysics Conference on High Energy Physics", Geneva 1991.